Chinese Physics C

Physical design of positronium time of flight spectroscopy apparatus[*]

JIANG Xiao-Pan(姜小盼)[1,2]   ZHANG Zi-Liang(张子良)[3]   QIN Xiu-Bo(秦秀波)[1]

YU Run-Sheng(于润升)[1]   WANG Bao-Yi(王宝义)[1;1)]

[1] Key Laboratory of Nuclear Analysis Techniques, Institute of High Energy Physics, CAS, Beijing 100049, China
[2] Graduate University of Chinese Academy of Sciences, Beijing 100049, China
[3] College of Applied Nuclear Technology & Automation Engineering,
Chengdu University of Technology, Chengdu 610059, China

Abstract   Positronium time of flight spectroscopy (Ps-TOF) is an effective technique for porous material research. It has advantages over other techniques for analyzing the porosity and pore tortuosity of materials. This paper describes a design for Ps-TOF apparatus based on the Beijing intense slow positron beam, supplying a new material characterization technique. In order to improve the time resolution and increase the count rate of the apparatus, the detector system is optimized. For 3 eV o-Ps, the time broadening is 7.66 ns and the count rate is 3 cps after correction.

Key words   positronium time of flight spectroscopy (Ps-TOF), positron annihilation, plastic scintillator, time broadening, count rate

PACS   42.15.Eq

1   Introduction

Positronium time of flight spectroscopy (Ps-TOF) is an effective technique for porous material research. It has advantages over other techniques for analyzing the porosity and pore tortuosity of materials. KEK [1], Tokyo university [2], Lawrence Livermore National Laboratory (LLNL) [3] and some other institutes have constructed Ps-TOF apparatus.

Much work has been done by using the Ps-TOF technique. KEK measured the TOF of the Ps emitted from single-crystal and amorphous silicon oxide using a high-intensity pulsed positron beam, and the data indicate that a Ps is emitted by two mechanisms: the emission of Ps formed in the bulk, and Ps formation on the surface with energies of 1 and 3 eV, respectively [1]. R. S. Yu et al. studied a series of porous low-k films by Ps-TOF spectroscopy, and the data definitely indicate the porosity and pore tortuosity of the films [4].

When entering the samples, the positron freely annihilates with an electron, or binds with an elec-

tron to form a positronium (Ps) with a vacuum binding energy of ~ 6.8 eV. The singlet $^1S_0$ state (para-positronium, or p-Ps) has a vacuum lifetime of approximately 125 psec, and it decays predominantly into two γ rays of ~ 511 keV energy. Its total spin is $S = 0$ ($m_s = 0$), as opposed to that of the triplet $^3S_1$ state (ortho-positronium, or o-Ps), which has a total spin $S = 1$ ($m_s = 0, +1, -1$). The lifetime of o-Ps is about 142 nsec, and in vacuum it decays into three or more γ rays [5].

The Beijing slow positron beam [6–9] is based on a 50 mCi ^{22}Na source or linac, and transported by a 100 G uniform axial magnetic field produced by Helmholtz coils. When based on the ^{22}Na source mode, the intensity of the positron beam is 10^5 e$^+$/s. The Doppler broadening of annihilation radiation (DBAR) and the positron annihilation lifetime spectroscopy (PALS) have been constructed and run normally. This paper describes the physical design of positronium time of flight spectroscopy apparatus based on the Beijing slow positron beam.

In this paper, all of the parameters' units are in-

ternational units, unless otherwise stated.

In Fig. 1, R is the radius of the transport pipe, d is the axial distance between the middle of the slit and the sample, and a and b refer to the width and height of the slit, respectively. A plastic scintillator is placed behind the slit to detect the γ rays produced by o-Ps annihilation. Pb is placed around the slit to shield the γ rays produced by the prompt annihilation, including positron free annihilation with electrons and p-Ps annihilation, and the γ rays produced by the annihilation in the unsuitable places are also shielded.
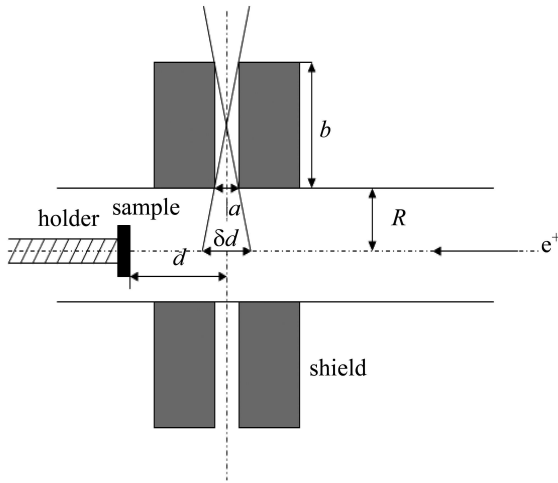
Fig. 1.   A schematic diagram of the Ps-TOF system.

δd is the axial distance of the slit broadening along the transport line. Positronium time of flight spectroscopy is the relationship between the o-Ps time of flight and the count of γ rays produced by the o-Ps annihilation. For the Beijing slow positron beam, the time start signal is given by the chopper, while the stop signal is given by the photomultiplier tube, from which the time interval is obtained.

When the positrons enter the samples (mainly porous materials and polymers), they form o-Ps with electrons. After emitting into the pore, o-Ps continuously loses energy by colliding with the pore wall until it is emitted from the sample surface into the vacuum. In the design, the time interval between the o-Ps emission from the sample surface and the annihilation at an appropriate position is considered.

After emitting into vacuum from the sample surface, o-Ps flies at a constant speed until annihilation. The time of flight is expressed as

$$T = \frac{d}{v} = \frac{d}{\sqrt{\dfrac{2E_{\text{o-Ps}}}{M}}} = \frac{d}{\sqrt{\dfrac{E_{\text{o-Ps}}}{m_{\text{e+}}}}}, \tag{1}$$

where T is the time of flight, d is the distance of flight, v is the speed of flight, $E_{\text{o-Ps}}$ is the kinetic energy of the o-Ps, and $m_{\text{e+}}$ is the mass of the positron.

In order to optimize the time resolution and count rate, the transport pipe radius R, the slit width a, the slit height b, and the shape and size of plastic scintillator were considered seriously.

2   Transport pipe radius

The transport pipe radius influences the resolution of the Ps-TOF apparatus. As shown in Fig. 1, according to the geometry, the following equation is deduced,

$$\delta d = \frac{2a(b+R)}{b} - a. \tag{2}$$

In the same slit width and height situation, with the transport pipe radius increasing, the apparatus resolution and the shield efficiency became worse. In the design, considering the pipe link with the original apparatus and the relation between the time resolution and the transport pipe size, the transport pipe radius R was set to be 30 mm.

3   Slit width and height

Emitting from the surface of certain materials, o-Ps represents the peaks in Ps-TOF spectroscopy. For porous silicon oxide, Ps-TOF spectroscopy shows two peaks: one is 3 eV and the other is 1 eV [10]. After substitution $E_{\text{o-Ps}}$ and $m_{\text{e+}}$ by the exact data, Table 1 is deduced.

Table 1.   Time of flight and time broadening of different energies o-Ps.

$E_{\text{o-Ps}}$/eV	T/μs	δT/μs
1	2.38d	2.38δd
3	1.37d	1.37δd

This paper used $E_{\text{o-Ps}} = 3$ eV to decide the resolution of the apparatus. From Table 1,

$$\delta T = 1.37\delta d. \tag{3}$$

From Eqs. (2) and (3), the time broadening δT in different a (slit width) and b (slit height) was calculated, and Geant4 [11] software was used to simulate and estimate the efficiency of the γ rays produced by o-Ps annihilation at the intersection point of the slit middle axes and the transport line passing through the slit. R was 30 mm, a varied from 1 mm to 5 mm

and b varied from 10 mm to 100 mm. From the simulation data, $a = 3$ mm, $b = 70$ mm, $a = 2$ mm, $b = 40$ mm made the time broadening less than 8 ns and the efficiency more than 0.3%. For the latter, the slit height was too short, which caused a decrease in the apparatus shield efficiency. Thus, a was set to be 3 mm and b was set to be 70 mm, and then δT was calculated to be 7.63 ns, and the efficiency of the γ rays passing through the slit was calculated to be 0.318%.

4 Shape and size of the plastic scintillator

For the collection of γ rays, the apparatus time resolution requires the ns scale, and the decay time of the plastic scintillator ranges from 1 ns to 3 ns, which meets the requirement. Compared with the inorganic scintillator, the plastic scintillator is more convenient to process, and the cost is less. BC-418 is chosen, and its density is 1.032 g/cm³, the refractive index is 1.58, the spectra peak is at 391 nm, the decay time is 1.4 ns and the attenuation length is 100 cm.

The intensity of the slow positron beam based on a ²²Na source is 10^5 e⁺/s, and the yield of o-Ps is about 10^4/s [12]. The effect of o-Ps intrinsic decay is corrected by the coefficient exp $(t/142$ ns), and the efficiency of the γ rays produced by o-Ps annihilation passing through the slit is about 30 cps. In order to collect them as far as possible and increase the apparatus count rate, the shape of the plastic scintillator needs to be optimized, which reflects the light to the photomuitplier tube as much as possible. Moreover, the optical path difference in the plastic scintillator influences the apparatus time resolution, and in the design, the optical path difference needs to be decreased as much as possible.

The photons are emitted around 4π solid angle, and the design aims to collect the light absolutely by the photomultiplier tubes as little as possible. In order to optimize the collection efficiency and decrease the optical path difference, a four-detector system was adopted, and each detector collected photons emitted around π solid angle. The shape of the plastic scintillator was optimized, and more reflecting planes were provided so as to assist the light reflection, which led to the absolute light collection as shown in Fig. 2.

Figure 2 shows a schematic diagram of one fourth section, and it has two concentric circles: the inner is the transport pipe and the outer is the Pb shield. The line HL is the upside of the scintillator, which is assembled with the photomuitplier tube by means

of the light guide, and the line JP is the thickness of the part of the plastic scintillator which is near the upside HL. Fixing HL and OA, and assigning the value of the downside AB to 5 cm, from the light path there are four transport modes to the upside HL for the light emitted from the origin O.
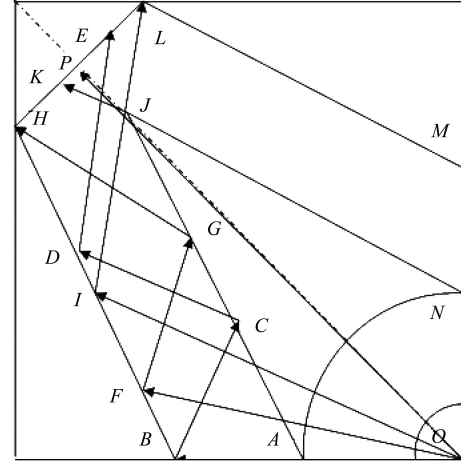
Fig. 2. A schematic diagram of the shape of the plastic scintillator and the light path.

Table 2. Light path of plastic scintillator downside $AB = 5$ cm.

reflection times	longest light path/cm	shortest light path/cm
0	22.825	21.9
1	34.2339	22.825
2	31.4373	29.9039
3	48.2995	31.4373

From Table 2, the longest and the shortest light paths are 48.2995 cm and 21.9 cm, respectively. The refractive rate of BC-418 is 1.58, and based on the equation $v = c/n$, the velocity of photons is calculated to be 1.9×10^8 m/s. For the longest light path, the distance of light transport in the plastic scintillator is 38.2995 cm, and that in the air is 10 cm, so the total light transport time is

$$T = \frac{L1}{v} + \frac{L2}{c} = 2.02 \text{ ns} + 0.33 \text{ ns} = 2.35 \text{ ns}. \quad (4)$$

For the shortest light path, the distance of light transport in the plastic scintillator is 2.4 cm, and that in the air is 19.5 cm, so the total light transport time is

$$T = \frac{L1}{v} + \frac{L2}{c} = 0.13 \text{ ns} + 0.65 \text{ ns} = 0.78 \text{ ns}. \quad (5)$$

The time broadening caused by the difference between the longest and shortest light path is

$$\delta T = 2.35 \text{ ns} - 0.78 \text{ ns} = 1.57 \text{ ns}. \quad (6)$$

Assigning the value of the downside AB to 1, 2, 3 and 4 cm respectively, the corresponding time broadening and JP thickness can be calculated as shown in Fig. 3 and Fig. 4.

Figure 3 shows that, with the downside width of the plastic scintillator AB decreasing, the time broadening caused by the different light path in the plastic scintillator also decreases, whereas the JP thickness increases. The increase in JP thickness results in the waste of materials, and the self absorption of the plastic scintillator results in a disadvantage for fluorescence photon detection. The energies of the γ rays produced by o-Ps annihilation range from 0 to 511 keV, and the interaction between the γ rays in that energy range and the plastic scintillator is mainly Compton scattering. The energies of the electrons produced by Compton scattering range from 0 to
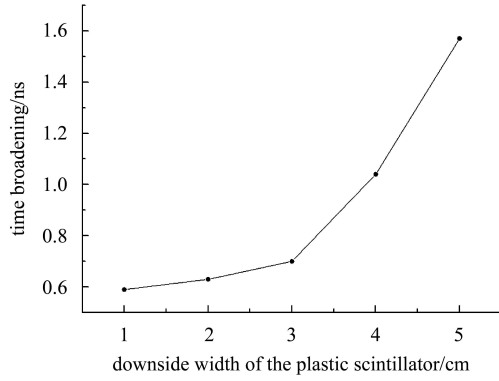
Fig. 3.   Time broadening in the different downside widths of the plastic scintillator.
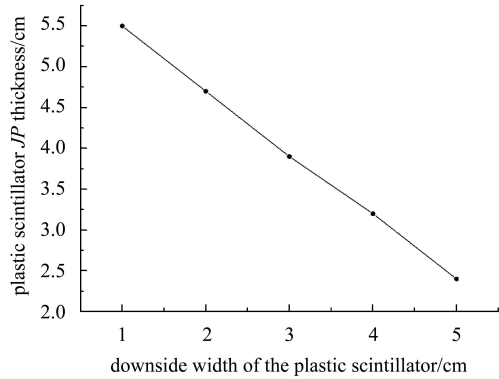
Fig. 4. JP thickness in the different downside widths of the plastic scintillator.

341 keV [12]. In order to keep the energy of the γ rays as much as possible, and considering the time broadening and the count rate, the downside of the plastic scintillator $AB = 3$ cm, $\delta T = 0.7$ ns and $JP = 3.9$ cm. The total time broadening of the apparatus is

$$\delta T' = \sqrt{7.63^2 + 0.7^2} = 7.66 \text{ ns.} \tag{7}$$

Because a part of scintillator is away from the slit, the thickness of the plastic scintillator is calculated in order to avoid losing count.
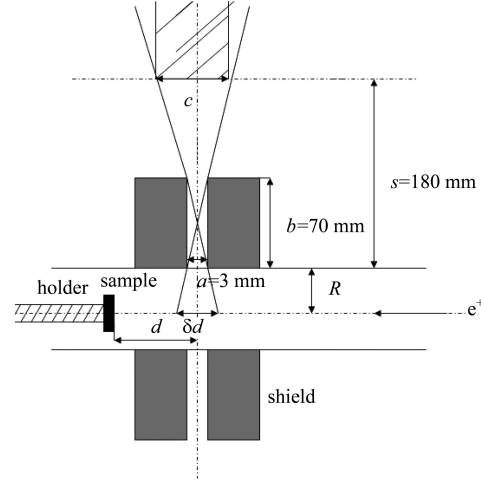
Fig. 5.   The schematic diagram of calculating the thickness of the plastic scintillator.

As shown in Fig. 5, according to the geometry, the following equation can be deduced,

$$\frac{a}{b} = \frac{a/2 + c/2}{s}. \tag{8}$$

The thickness of the scintillator $c = 12.43$ mm was obtained, and in the real assembly, $c = 12.5$ mm is adopted.

5   Conclusion

This paper introduces the physical design of positronium time of flight spectroscopy apparatus, the time broadening and count rate are calculated, and the parameters of the apparatus are optimized. For 3 eV positronium, the time broadening is 7.66 ns. After correction and optimization, the mean count rate is 3 cps based on the efficiency of the photomultiplier tube (10%).

References

1　Kurihara T, Yagishita A, Enomoto A et al. Phys. Rev. B, 2000, **171**: 164–171

2　Mondal N N, Hamatsu R, Hirose T et al. Applied Surface Science, 1999, **149**: 269–275

3　Tuomisaari M, Howell R H, McMullen T et al. Phys. Rev. B, 1989, **40**: 2060–2069

4　YU R S, Ohdaira T, Suzuki R et al. Appl. Phys. Lett., 2003, **83**: 4966–4968

5　YU Wei-Zhong. Principles and Applications of Positron Annihilation. Beijing: Science Press, 2003 (in Chinese)

6　CAO Xing-Zhong et al. HEP & NP, 2004, **28**(5): 560–563 (in Chinese)

7　CAO Xing-Zhong et al. Nuclear Science and Techniques, 2004, **27**(6): 435–439 (in Chinese)

8　WANG Bao-Yi, YU Wei-Zhong et al. BSRF Annals, 2000, (1): 276–277 (in Chinese)

9　WANG Ping et al. HEP & NP, 2006, **30**(10): 1036–1040 (in Chinese)

10　Nagashima Y, Morinaka Y, Kurihara T et al. Phys. Rev. B, 1998, **58**: 12676–12679

11　GEANT-Detector Description and Simulation Tool, CERN Program Library, CERN Geneva, Switzerland

12　TENG Min-Kang. Spectroscopy and Applications of Positron Annihilation. Beijing: Atomic Energy Press, 2000. 21–47 (in Chinese)